Caracterización del transporte turbulento de partículas y optimización del calentamiento del plasma y la regulación de la corriente eléctrica en las bobinas del Stellarator SCR-1

Characterization of turbulent transport of particles and optimization of plasma heating and operation current control in the coils of the SCR-1 Stellarator

Ricardo Solano-Piedra[1], Luis Alonso Araya-Solano[2],Ana María Murillo-Morgan[3], José Esteban Pérez-Hidalgo[4], Iván Vargas-Blanco[5], José Andrés Borloz-Chinchilla[6], Robert David Cerdas-Bermúdez[7], Manuel Antonio Bojorge-Araya[8], Julián David Sánchez-Castro[9], David Fabián Díaz-Sánchez[10], Kendy Raquel Arias-Ortiz[11]

Fecha de recepción: 28 de octubre, 2025
Fecha de aprobación: 21 de febrero, 2026

Caracterización del transporte turbulento de partículas y optimización del calentamiento del plasma y la regulación de la corriente eléctrica en las bobinas del Stellarator SCR-1. *Tecnología en Marcha*. Vol. 39 Nº 3. Julio-Setiembre, 2026. Pág. 115-131.

https://doi.org/10.18845/tm.v39i3.8275

1 Plasma Laboratory for Fusion Energy and Applications. School of Physics, Costa Rica Institute of Technology, Costa Rica. risolano@itcr.ac.cr https://orcid.org/0000-0003-3092-8654
2 Plasma Laboratory for Fusion Energy and Applications. School of Physics, Costa Rica Institute of Technology, Costa Rica. luaraya@itcr.ac.cr https://orcid.org/0000-0002-7941-821X
3 Plasma Laboratory for Fusion Energy and Applications. School of Mechatronics Engineering, Costa Rica Institute of Technology, Costa Rica. amurillo@itcr.ac.cr https://orcid.org/0009-0000-5805-4122
4 Plasma Laboratory for Fusion Energy and Applications. School of Physics, Costa Rica Institute of Technology, Costa Rica. jose.perez@itcr.ac.cr https://orcid.org/0009-0000-5805-4122
5 Plasma Laboratory for Fusion Energy and Applications. School of Physics, Costa Rica Institute of Technology, Costa Rica. ivargas@itcr.ac.cr https://orcid.org/0000-0001-9568-1598
6 Plasma Laboratory for Fusion Energy and Applications, Costa Rica Institute of Technology, Costa Rica. andres.borloz@estudiantec.cr https://orcid.org/0009-0004-9357-3621
7 Plasma Laboratory for Fusion Energy and Applications, Costa Rica Institute of Technology, Costa Rica. robertcerdas@estudiantec.cr https://orcid.org/0009-0001-4360-2904
8 Plasma Laboratory for Fusion Energy and Applications, Costa Rica Institute of Technology, Costa Rica. mbojorge@estudiantec.cr https://orcid.org/0009-0004-6071-5945
9 Plasma Laboratory for Fusion Energy and Applications, Costa Rica Institute of Technology, Costa Rica. jsanchezitcr@proton.me https://orcid.org/0009-0006-4787-4225
10 Plasma Laboratory for Fusion Energy and Applications, Costa Rica Institute of Technology, Costa Rica. fadiaz0123@estudiantec.cr https://orcid.org/0009-0001-6101-5009
11 Plasma Laboratory for Fusion Energy and Applications, Costa Rica Institute of Technology, Costa Rica. kendyarias@estudiantec.cr https://orcid.org/0009-0001-0359-8699

Keywords

Stellarator; ECRH; Turbulent transport; electrode biasing; Buck DC-DC converter; Vlasov antenna.

Abstract

The SCR-1 stellarator, operational since June 2016, has emerged as a pioneer in Latin America in the field of modular stellarator devices, developed by the Costa Rica Institute of Technology. This device has been the subject of continuous characterization and optimization efforts, with a focus on significant improvements in turbulence, coil feeding and wave propagation within the SCR-1 stellarator. This work presents a first study of turbulence, examining behavior at the plasma edge and its interaction with external electric fields, as well as the importance of electrode polarization. In addition, the design of the DC-DC Buck converter for the SCR-1 current coil control system is addressed, along with the proposal of a Vlasov antenna to optimize energy deposition in the plasma. Results indicate the significant influence of electrodes on plasma behavior. A power converter was designed to ensure an efficient and safe electrical supply and simulated by PLECS. The buck converter was deemed crucial for precise and stable current regulation in the coils. Electronic components were sized to handle the required current and voltage specifications. Finally, a modified Vlasov antenna was designed, which demonstrated in COMSOL multiphysics simulations that the new configuration improved the distribution of electromagnetic waves in the SCR-1 vacuum vessel.

Palabras clave

Stellarator; ECRH; Transporte turbulento; polarización de electrodos; convertidor Buck DC- DC; antena Vlasov.

Resumen

El stellarator SCR-1, operativo desde junio de 2016, ha surgido como un pionero en América Latina en el campo de los dispositivos stellarator modulares, desarrollado en el Instituto Tecnológico de Costa Rica. Este dispositivo ha sido objeto de continuos esfuerzos de caracterización y optimización, con un enfoque en mejoras significativas en turbulencia, alimentación de bobinas y propagación de ondas dentro del stellarator. Este trabajo presenta un primer estudio sobre la turbulencia, examinando su comportamiento en el borde del plasma y su interacción con campos eléctricos externos, así como la importancia de la polarización de los electrodos. Además, se aborda el diseño de un convertidor Buck DC-DC para el sistema de control de corriente de las bobinas del SCR-1, junto con la propuesta de una antena tipo Vlasov para optimizar la deposición de energía en el plasma. Los resultados indican una influencia significativa de los electrodos en el comportamiento del plasma. Se diseñó un convertidor de potencia para garantizar un suministro eléctrico eficiente y seguro, el cual fue simulado en PLECS. El convertidor Buck se consideró crucial para la regulación precisa y estable de la corriente en las bobinas. Los componentes electrónicos fueron dimensionados para manejar las especificaciones requeridas de corriente y voltaje. Finalmente, se diseñó una antena Vlasov modificada, la cual demostró mediante simulaciones en COMSOL Multiphysics que la nueva configuración mejoró la distribución de las ondas electromagnéticas dentro de la cámara de vacío del SCR-1.

Introduction

Operational since June 2016, the SCR-1 Stellarator, a groundbreaking device in Latin America, was designed, built, and operational at the Costa Rica Institute of Technology. Initially, the project focused on overcoming the engineering challenges associated with developing a compact magnetic confinement device. The SCR-1 is characterized by a two-field period modular design, a major radius of 247.7 mm and an aspect ratio of 6.2, with a low-shear magnetic configuration. Its vacuum vessel is made from 6061 - T6 aluminum and has 12 modular coils, each with 6 turns, carrying 725 A per turn, resulting in a toroidal field current of 4.35 kA turn per coil. These coils are powered by a 120 V battery bank, and plasma is generated providing 2 kW at 2.45 GHz, corresponding to the second harmonic (B = 43.8 mT). The plasma pulses last between 4s to 10s, with a minor radius of 39.95 mm, a plasma volume of 0.0078 m^3, an average electron density of 5 x 10^{15} m^{-3}, and an electron temperature of 6 eV to 14 eV [1]. In this new phase of applied development for the SCR-1 stellarator, efforts are focused on further characterizing and optimizing the magnetic confinement device and the plasma it produces.

This research aims to delve deeper into the behavior of turbulence and transport at the edge of the confined plasma, as well as analyze the interaction of externally generated radial electric fields with these turbulent modes. Therefore, the research hypothesis is that the implementation of a radial electric field through external biasing can induce a sheared poloidal flow, thereby suppressing edge turbulence and improving particle confinement. To test this, the study defines the following general objective: to characterize particle transport and turbulence in the SCR-1 through the optimization of plasma heating and the precise regulation of electrical current in the modular coils. The specific objectives of the study are: i) determine particle transport and turbulence levels in the SCR-1 plasma; ii) establish the nature of turbulence and its control through external electric fields; iii) develop a power conversion system to regulate coil current with automated safety and cooling features; and, iv) implement a modified Vlasov antenna to optimize energy deposition in the plasma.

In the periphery of fusion devices, a significant challenge arises due to the increased loss of particles and energy. The efficiency of stellarators is considerably reduced as these enhanced edge losses degrade the confinement conditions. At the edge, magnetic field lines spread out, and the plasma vigorously interacts with neutral particles, directly impacting its particle and energy balance. Investigating the plasma edge is essential for understanding the overall plasma behavior and improving the performance of fusion devices. Both the edge and the Scrape-Off Layer (SOL) typically exhibit turbulent structures and electrostatic fluctuations. These phenomena dominate particle and energy losses, significantly limiting the overall confinement conditions [2].

In this context, various edge studies conducted on devices with different parameters aim to comprehensively understand the physical processes generating edge turbulence and the constraints they impose on plasma confinement. Losses in Tokamak devices are not continuous but occur intermittently due to the radial convection of turbulent structures known as filaments or “blobs” [3]. These fluctuations exhibit intermittent behavior with short lifetimes, allowing them to appear and disappear at the plasma edge within microseconds. The formation and movement of these blob filaments result in electrostatic fluctuations in various plasma parameters. This includes the plasma electron density, $\tilde{n}_e(t)$, and the radial velocity of the charged particles in the plasma, $\tilde{v}_r(t)$. The tilde denotes the fluctuations of a given quantity over time, expressed as:

$$\tilde{n}_e(t) = n_e(t) - \langle n_e \rangle \quad (1)$$

where $\langle n_e \rangle$ is the time-averaged value. In this study, the ion saturation current ($\tilde{I}_s$) is used as a proxy for electron density ($\tilde{n}_e$). This is justified because $\tilde{I}_s$ is measured when the probe potential is sufficiently negative to repel all electrons, making the collected current proportional to the local plasma density.

The turbulent radial flux (Γ_r) is derived from the correlation between fluctuations in density ($\tilde{n}_e$) and radial velocity ($\tilde{v}_r$), which can be expressed through experimental proxies. Anomalous levels of net radial transport arise from the correlated fluctuations in plasma density and radial velocity, given by:

$$\Gamma_r \simeq \langle \tilde{n}_e \tilde{v}_r \rangle \propto \frac{\langle \tilde{I}_s \tilde{E}_\theta \rangle}{B} \tag{2}$$

$$\tilde{E}_\theta = -\frac{\Delta \tilde{V}_f}{d} \tag{3}$$

$$v_r^{eff} = \frac{\langle \tilde{I}_s \tilde{E}_\theta \rangle}{I_s B} \tag{4}$$

$$v_\theta^{ph} = \frac{\tilde{E}_r}{B} \tag{5}$$

where Γ_r is the turbulent radial flux, $\tilde{E}_\theta$ is the poloidal electric field, v_r^{eff} is the radial effective velocity, v_θ^{ph} is the poloidal phase velocity, I_s is the ion saturation current, B is the magnitude of the magnetic field, $\Delta \tilde{V}_f$ is the floating potential difference, d is the distance between the electrode with the external electric field and the reference electrode, and $\tilde{E}_r$ is the radial electric field [4]. A radial electric field has the potential to cause notable changes in particle trajectories. It initiates a poloidal drift along the flux surface, influencing the particle's poloidal velocity in such a way that both components counterbalance each other. As a result, particles maintain a fixed poloidal position and exhibit behavior akin to particles following helical paths. This phenomenon also leads to a decrease in ion saturation current and the radial velocity of charged particles [5].

Achieving higher beta values in confined plasma requires precise control of the current supplied to the coils. This necessitates a regulated power supply for the external coil system that generates the magnetic field. The choice of converter depends on the primary power source: DC (battery bank) or AC (three-phase). The Buck Converter is a popular choice due to its simplicity and cost-effectiveness. However, employing this converter for high-power scenarios with currents exceeding 800 A poses a significant challenge. Careful consideration is required when activating MOSFET power elements to prevent component damage. When employing a battery bank as the primary power source, a protection system is crucial. This system should include a manually and remotely disconnectable magnetothermal circuit breaker and an arc protection chamber for the contacts. Circuit breakers can withstand short-circuit current overloads, as the magnetic element activates the protective circuit without delay. A high-power contactor with remote activation will serve as the connection/disconnection medium. Contactors are electrical switches designed for high-power circuits, capable of handling substantial current intensities [6].

The electron cyclotron resonance heating system for the SCR-1 stellarator includes a microwave isolator to protect the magnetron and a directional coupler that records measurements of reflected power and transmitted power during the discharge. The radiation is then directed to a triple stub tuner, which is responsible for coupling the radiation to the plasma by selecting the minimum possible reflection coefficient. Finally, a waveguide with a quartz window, having a surface flatness of half the wavelength, is used to minimize the impedance of the electromagnetic waves [7]. Designing an optimal internal antenna (within the vacuum vessel) that adheres to the dimensional and design constraints is crucial. The antenna design involves a waveguide cut at a specific angle. This antenna will be installed within the vacuum vessel, requiring meticulous consideration of several constraints. Notably, the end of the antenna facing the plasma must avoid contact to prevent damage, necessitating precise dimension calculations. Studies have considered these factors, as noted in [8].

Furthermore, the limited space between the SCR-1 vacuum vessel wall and the plasma boundary presents a significant challenge, calling for a thorough analysis of the constraints that will define the feasible configurations of the antenna; a similar situation happens for TJ-K stellarator [9]. Therefore, Vlasov antennas are a good choice. Vlasov antennas are made up of a cylindrical waveguide with a cutoff, which allows them to radiate energy in cylindrical symmetry modes with circular guide waves, without requiring an additional mode converter. The Vlasov antenna presents versatility when making modifications, these can be varying the cut angle for a simple antenna, making a different crosscut or adding a reflector to the antenna, in the same way, it is important to consider its handling so that it does not have sharp edges that could damage the equipment or be dangerous when handling it [10, 11].

Materials and methods

Experimental Turbulence Measurement

For plasma turbulence measurements, an electrode was necessary to generate an external electric field. The electrical circuit design for the electrode aimed to meet specific requirements, including frequency variation between 100 Hz and 2000 Hz, variable voltage amplitude around 100 V, and the generation of sinusoidal waveform oscillating between 0 V and negative values. To address the complexity of precise frequency oscillation and amplitude adjustments, a function generator was utilized. While this device enabled waveform generation within the required frequency range, it had limitations in amplitude values. To overcome this limitation, a transformer amplified the output signal, ensuring it met the desired voltage amplitude. An offset was applied to ensure waveform oscillation between negative values.

The experimental setup of the Langmuir probe placed in the SCR-1 stellarator at the Plasma Laboratory for Fusion Energy and Applications is depicted in Figure 1. The outputs of the Langmuir probe tips were connected to the electrode circuit and data collection tips, such that one tip acted as the electrode while another performed data collection. The power supply and required frequencies for the electrode circuit were obtained from the depicted power sources and frequency generator.

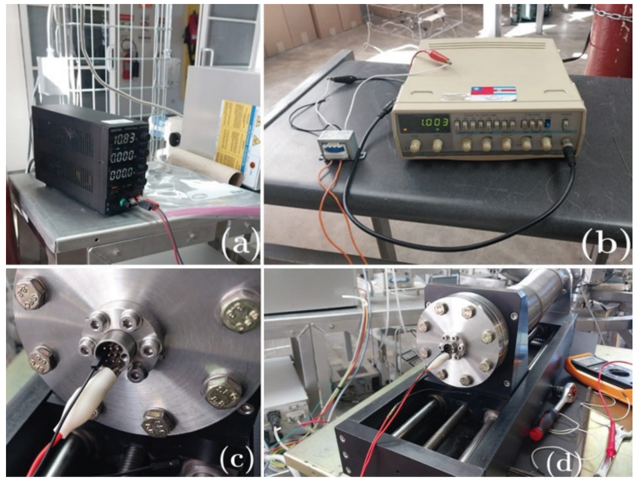

Figure 1. Experimental setup of Langmuir probe in the SCR-1 stellarator: (a) voltage source, (b) signal generator, (c) connections to the Langmuir probe, and (d) panoramic view of connections to the Langmuir probe.

To measure ion saturation current and floating potential, Langmuir probe current-voltage curves were obtained with a sampling frequency of 1500 samples/s. The voltage sweep ranged from -80 V to 10 V. The positioning of the Langmuir probe tip was determined using the BS-SOLCTRA magnetic field code [12]. Measurements were conducted at three radial positions: R = 0.2905 m, R = 0.3070 m and R = 0.3151 m, while maintaining a constant vertical position of z = -0.0125 m as shown in Figure 2. SCR-1 plasma discharges were conducted in three modes: without the electrode, with the electrode at - 60 V, and with the electrode at - 120 V. The data analysis is available in the PlasmaTEC-ITCR repository on GitLab. The turbulence important parameters Γ_r, $\tilde{E}_\theta$, v_r^{eff} and v_θ^{ph}, equations (2) to (5), were then calculated based on the processed data.

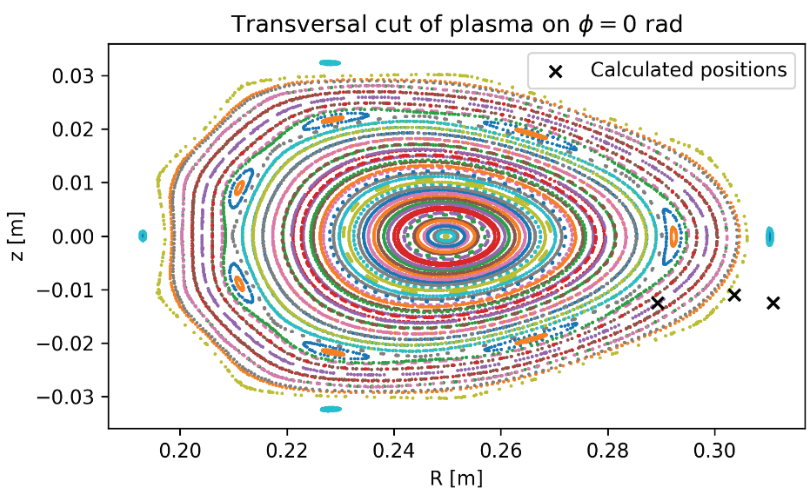

Figure 2. Magnetic flux surfaces for 0° toroidal position and calculated positions for Langmuir probe measurements.

Data was acquired using a National Instruments PXIe-8135 module with a sampling frequency of 1500 samples/s and a voltage sweep from −80 V to 10 V. Processing was performed via Jupyter Notebooks (Python) which employs a machine learning regression model to determine I_s, and identifies the floating potential $\Delta\tilde{V}_f$ where net current is zero. Noise was filtered, and the Grubbs' Test was applied with a significance level of $\alpha = 0.01$ to detect outliers.

Control coils current for the SCR-1 stellarator

The power system was modeled for 12 modular coils in series with a measured resistance of 0.08 Ω and an inductance of 3.9 μH. The Buck converter was designed with a 20 % duty cycle (D = 0.20) to step down a 293 V rectified input to a stable 58 V output. A PI Controller was integrated with an SG3525 PWM controller and a HAT 800-S Hall sensor to maintain a constant 725 A current per turn, regardless of load fluctuations caused by coil heating.

The control coils current system for the SCR-1 stellarator was designed to receive its main power supply from the electrical grid, which then reaches a three-phase transformer. This transformer will provide the necessary power for the SCR-1, but only after passing through the AC/DC conversion stage. Once rectified, the DC-DC conversion process adjusts the values to meet system requirements. Figure 3 shows the key stages for the system's power supply demand.

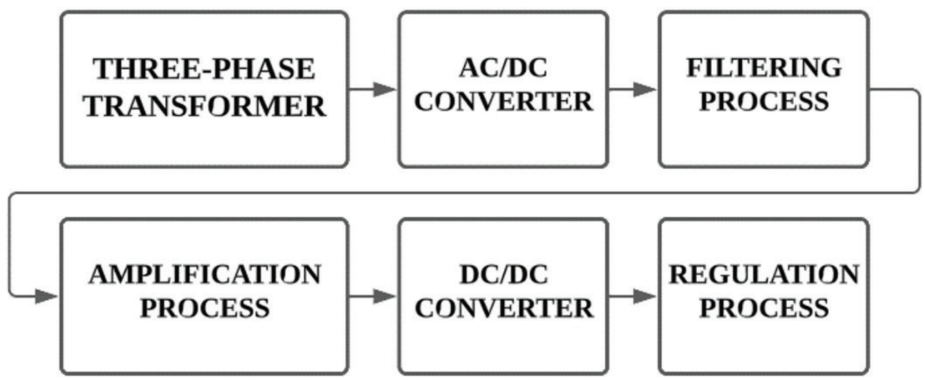

Figure 3. System power supply design diagram.

The SCR-1 coils, which are series connected, have a measured resistance of 0.08 Ω and an inductance of 3.9 μH, all of which comprise essential data for the design of the Buck converter. It is important to note that the temperature variation of the coils, ranging from 20 ºC to 70 ºC after 8.0 s of operation, is considered to ensure system stability, although its impact on electrical resistance is negligible, as stated by [14]. For this design, the process began with the rectification stage of the signal using an AC-DC converter. Power diodes and industrial-type capacitors were considered due to the high magnitude of current required by the SCR-1 stellarator during its operation. The proposed circuit is shown in Figure 4.

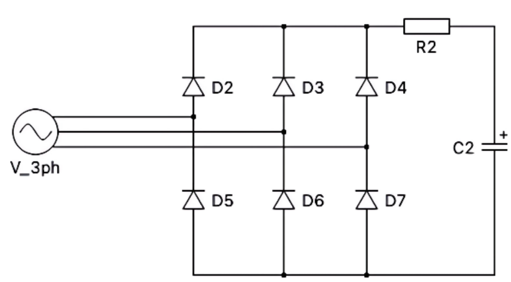

Figure 4. Proposed AC-DC converter circuit diagram.

For the simulation of the AC-DC converter circuit, PLECS software was employed, selected for its utility in engineering for designing and simulating power systems. PLECS is recognized for its speed, integration with Simulink, extensive component library, thermal modeling capabilities, and ease of use. The filter capacitor shown as C2 in Figure 4 was chosen considering the voltage and current it must withstand and the availability of components on the market, without omitting the fact that the rectifier ripple should be minimal, and for this work, a 3% ripple was considered appropriate. Considering the high current magnitude in the SCR-1, as well as a voltage of 120 V_{RMS} from the three-phase transformer, the following commercial electronic components were chosen for the implementation of the electrical circuit:

- Capacitor: MAL250034153E3 from manufacturer Vishay Beyschlag/Draloric/BC Components. This is an aluminum electrolytic capacitor with screw terminals, with a capacitance of 15 000 μF and a voltage rating of 420 VDC. Twelve capacitors must be used in parallel to achieve the capacitance of 180 000 μF.
- Rectifier Diodes: VS-SD400C04C from manufacturer Vishay Semiconductors. This is a rectifier diode with a direct current capacity of 800 A, a reverse voltage of 400 V, and a forward voltage of1.86 V.

The inclusion of resistor *R2* in Figure 4 is specifically intended to mitigate numerical errors during the simulation's initial stages. However, once the circuit is implemented, *R2* becomes superfluous and serves no practical function. To maintain a continuous current in SCR-1's coils, employing a buck converter was deemed suitable. The output voltage was set to 58V tailored to meet the precise specifications of the stellarator. The Buck converter was sized with a safety margin due to the experimental nature of the equipment. The diagram of the proposed circuit is shown in Figure 5.

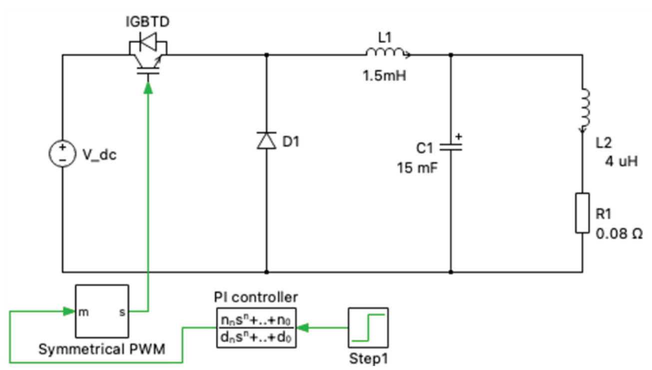

Figure 5. PWM and Buck converter circuit.

The Pulse Width Modulation (PWM) necessary for controlling the Insulated Gate Bipolar Transistor (IGBT) referred to as IGBTD in Figure 5, was simulated using a frequency generator represented as Symmetrical PWM within the same figure. Components *R1* and *L2* correspond to known values for the SCR-1 coils. The remaining components were sized according to general equations for a Buck converter circuit [15], considering component availability in the market Duty cycle *D* was calculated as a ratio between the output and input voltage of the rectifier, resulting in *D* = 0.2.

Inductor *L1* was selected through the following criteria. The coil is chosen based on market availability while ensuring it supports continuous conduction mode [15]. Choosing an inductance of 1.5 mH, the ripple current is calculated to validate it remains within a safe and acceptable range for the stellarator operation. Considering known values of V_0, V_1, and *D*, and estimating a switching frequency f of 2 kHz, the ripple current is:

$$\Delta I_L = \frac{(V_I - V_O)D}{Lf} \quad (6)$$

$$\Delta I_L = 15.67 \text{ A}$$

The obtained ripple current corresponds to approximately 2% of the circuit current, deemed acceptable for the application. The frequency value was set at 2 kHz to minimize switching losses; however, the frequency was also constrained by the values of capacitance and inductance of the filter, as choosing a lower frequency would result in higher component stresses, complicating commercial component selection. The output capacitor *C1* was selected considering the following. For design standardization, the same capacitor used in the current rectifier circuit was chosen. The output ripple voltage is:

$$V_O = \frac{\Delta I_L}{8fC} \tag{7}$$

$$V_O = 65.4\ \mathrm{mV}$$

Finally, the following commercial electronic components were chosen for circuit implementation:

- Power supply of 293 V VDC: corresponds to the current rectifier circuit output.
- IGBT (IGBTD): FZ1200R17HE4PHPSA1 from Infineon Technologies, with a maximum collector-emitter voltage of 1700 V and a continuous collector current of 1200 A.
- Diode (*D1*): VS-SD400C04C from Vishay Semiconductors, a rectifier diode with a direct current rating of 800 A, reverse voltage of 400 V, and forward voltage of 1.86 V.
- Capacitor (*C1*): MAL250034153E3 from Vishay Beyschlag/Draloric/BC Components, the same model used in the current rectifier circuit.
- Inductor (*L1*): DB2-154 from Gowanda Electronics, capable of handling currents up to 960 A and an inductance of 1.5 mH.
- To design a control system ensuring the PWM delivers a 58 V output in the Buck converter regardless of load variations, a feedback controller based on a PI controller in combination with the commercial PWM controller SG3525 from Texas Instruments was implemented. In the Buck converter, the PI controller adjusts the PWM duty cycle to maintain a constant output current. If the output current falls below the 725 A reference, a positive error increases the PWM duty cycle, thereby increasing the output current. Conversely, if the output current exceeds the reference, a negative error reduces the PWM duty cycle to decrease the output current. The transfer function for the Buck converter circuit is shown in the equation:

$$\frac{I_L(s)}{DV_{dc}(s)} = \frac{1}{L_1 L_2 C_1 s^3 + R_1 L_2 C_1 s^2 + (L_1 + L_2)s + R_1} \tag{8}$$

Vlasov antenna for the ECRH system

The COMSOL Multiphysics simulations utilized specific physical and geometric parameters to model wave propagation and heating within the SCR-1. The system was configured with a 2000 W power input at a frequency of 2.45 GHz provided by an Alter TMA2050 magnetron, operating in the TE10 mode. The simulation environment integrated multiple physics modules, including Electromagnetic Waves (frequency domain), Laminar Flow, Magnetic and Electric Fields (stationary), and a Plasma module using hydrogen gas and conductivity coupling. Geometric parameters were established for a Vlasov antenna located at the 330° toroidal port, ensuring its diameter was slightly smaller than the port and its length was sufficient to avoid contact with the plasma. The model employed an extra-fine mesh for the vacuum chamber and coils, while a fine mesh was applied to the external areas to balance precision and convergence. Finally, a parametric sweep was used to vary the antenna's cut angle α, specifically analyzing a 45° modified cut and an 81.4° bevel-cut to optimize electromagnetic wave deposition. Simulations were conducted in both frequency and stationary domains.

The design of the Vlasov antenna was developed using the COMSOL Multiphysics simulation program, where the following parameters were established for its development:

- Propagation mode of the wave incident on the SCR-1.
- Antenna diameter: it must allow the antenna to enter the port, being close enough to the diameter of the port to be considered as a single entity in the simulations.
- Length of the antenna inside the stellarator vacuum vessel: this dimension should ensure that the antenna inside the vacuum vessel does not touch the SCR-1 plasma.
- The cutting of the Vlasov antenna.
- The physics involved: it is described by electromagnetic waves, electric and magnetic fields, laminar flow, and plasma magnetic flux surfaces.

The Transverse Electric (TE) mode was chosen based on the design considerations for the ECR heating system, which favored the propagation of electromagnetic waves in the ordinary mode, as detailed in [16]. Consequently, the TE_{10} mode was utilized. Antenna diameter calculations were conducted using measurements taken by SOLIDWORKS software at the SCR-1 port in the toroidal direction of 330º, illustrated in Figure 6a, with the resulting measurements shown in Figure 6b. To determine the antenna's spatial allocation inside the SCR-1 vacuum vessel, the plasma model is overlaid, as depicted in Figure 7a. Subsequently, the available distance for the antenna inside the vacuum vessel, ensuring it does not contact the plasma, was measured, illustrated in Figure 7b.

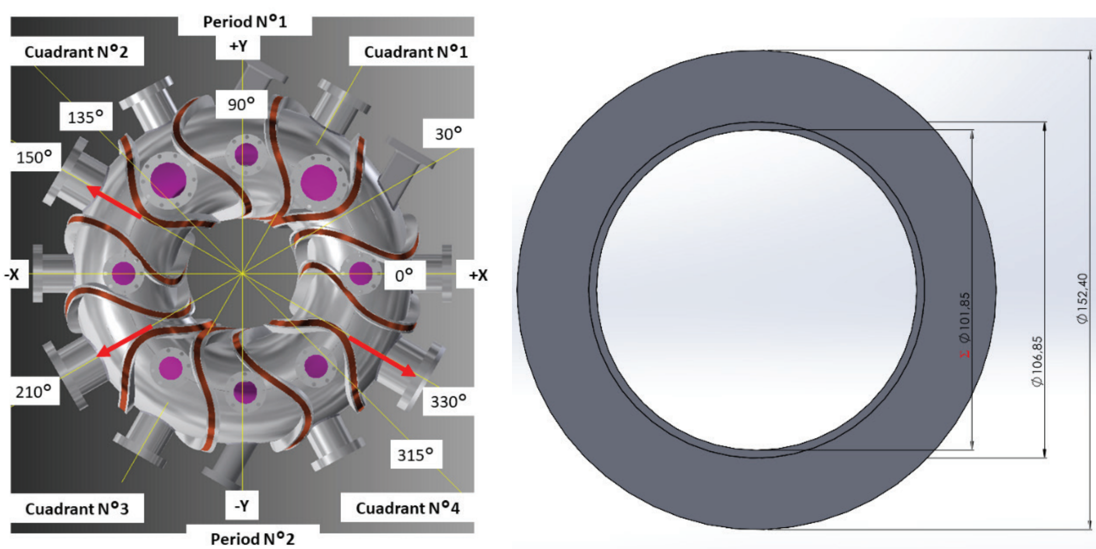

(a) (b)

Figure 6. (a) Top view of the Stellarator vacuum vessel with its ports.
(b) Rear view of the SCR-1 330º port in millimeters.

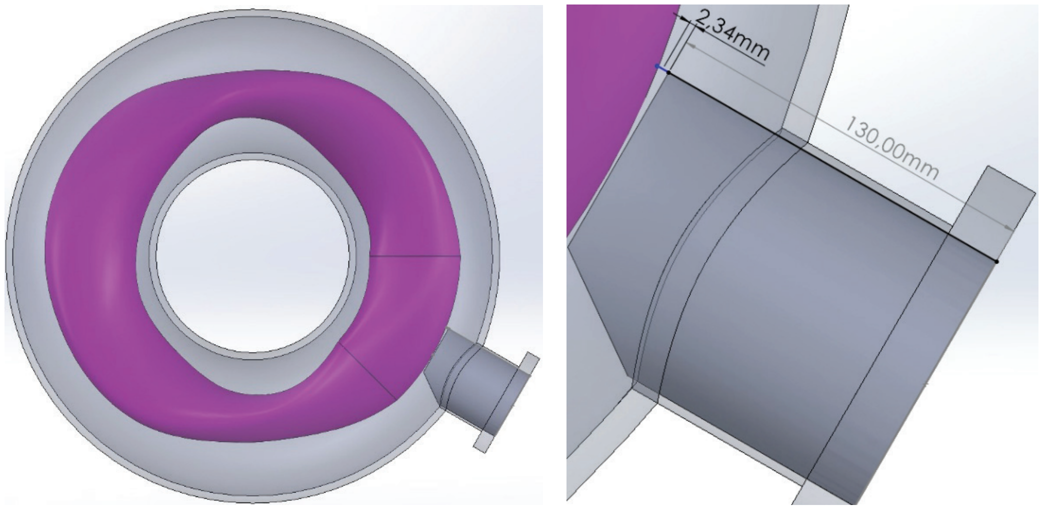

(a) (b)

Figure 7. (a) Top view of the Stellarator vacuum vessel with the plasma overlaid. (b) Desirable distance (millimeters) of the antenna without touching the plasma.

After completing the antenna measurements, a model was constructed and parameterized to vary the α angle in the simulation depicted in Figure 8. This involved using a parametric sweep with different cutting angles.

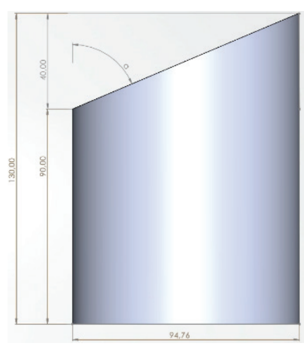

Figure 8. Proposed design of the dimensions (millimeters) of the Vlasov antenna.

Results

Plasma turbulence in the SCR-1 Stellarator

Significant observations were made regarding the impact of electrode introduction on plasma behavior in the SCR-1 stellarator. The changes in ion saturation current were consistent with expectations [5]; specifically, negative polarization led to a reduction in this current near the Last Closed Magnetic Surface (LCMS) and SOL, suggesting a lower electron density, as shown in Figure 9a. Although the radial variation was not mapped, preventing the determination of the SOL width, the flux values provided a reliable indicator for identifying where to continue mapping the region's width.

The radial velocity at R = 0.2905 m, as shown in Figure 9b, decreased markedly upon electrode introduction. A similar reduction was noted at R = 0.3070 m, a position closer to the last magnetic flux surface. Moreover, the poloidal velocity and electric field, illustrated in Figures 9c and 9d, exhibited a similar trend both with and without the influence of the electrode. However, during the critical phases of plasma discharge, between 1.5 s and 2.5 s, higher average values were observed, indicating maximum confinement during this period.

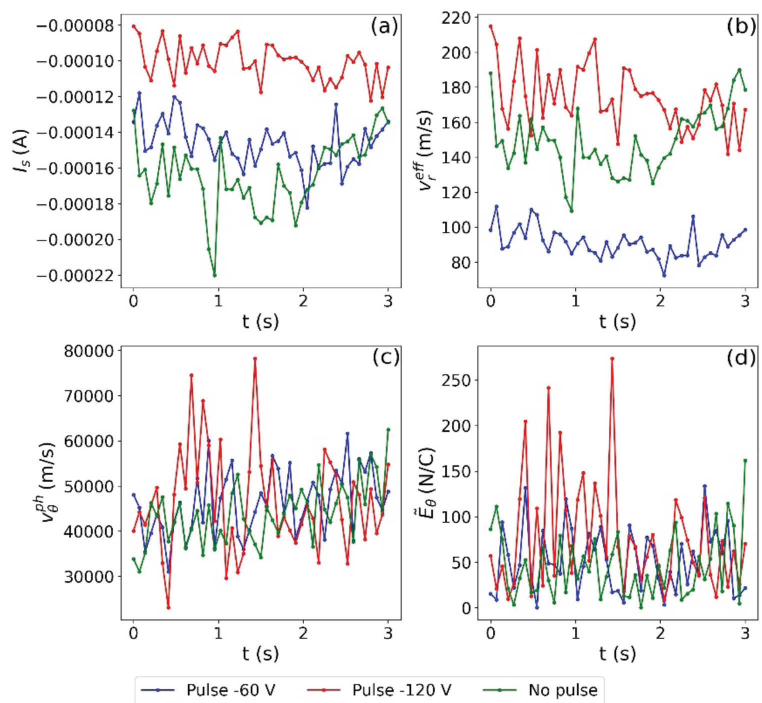

Figure 9. (a) Saturation ion current, (b) radial effective velocity, (c) poloidal velocity and (d) poloidal electric field in function of time for the radial position R = 0.2905 m.

The inclusion of the electrode resulted in a significant decrease in radial particle flux near the plasma, the generated electric potential enhanced the effective radial velocity of charged particles. Table 1 emphasizes a stronger radial flux near the edge compared to other locations where the magnetic field lines are closed and far from the confinement area. Furthermore, the electrode potential at - 120 V was observed to reduce radial flux, although less significantly than at - 60 V. Similar conclusions to those of our results were presented in [13].

Table 1. Radial particle flux as a function of electrode voltage and radial position.

Radial position r (m)	Electrode voltage V (V)	Radial flux Γ_r (a. u.)
0.2905	- 120	0.017
	- 60	0.013
	0	0.024
0.3070	- 120	0.039
	- 60	0.021
	0	0.045
0.3151	- 120	0.015
	- 60	0.016
	0	0.014

Control coils current for the SCR-1 stellarator

To measure the output current in the Buck circuit, it is proposed to use a Hall sensor HAT 800-S from LEM USA Inc, capable of measuring currents up to 800 A with an analog voltage output of ± 4 V Figure 10 illustrates the proposed power circuit for the SCR-1 coils, developed using the PLECS simulation software.

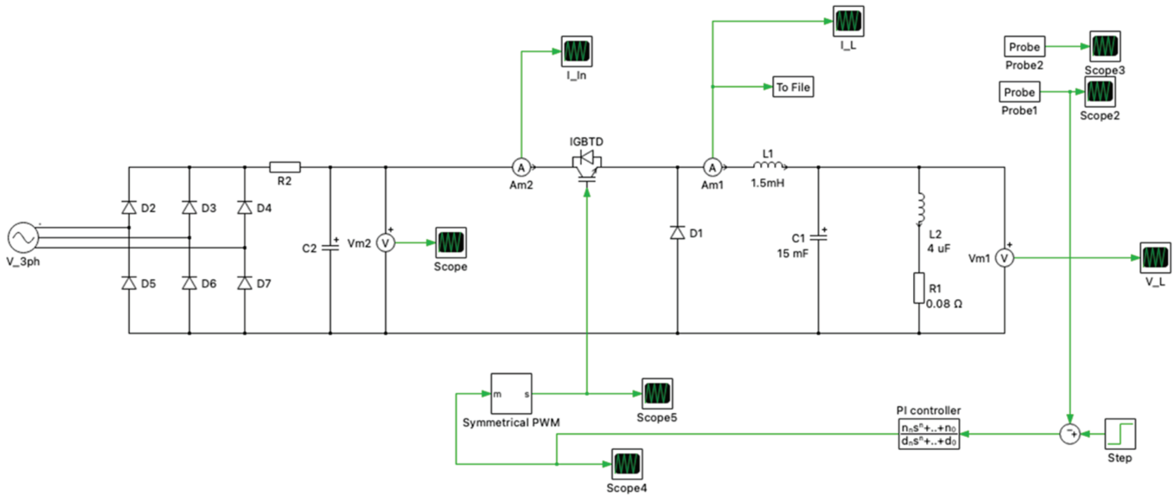

Figure 10. Power circuit for the SCR-1 coils obtained in the software PLECS.

Figure 11 shows different measurements at certain points of the circuit presented in Figure 10. Figure 11a shows the rectified wave at the output of the rectifier current circuit, measured at the voltmeter *Vm2*. Likewise, in Figure 11b the current at the output of the Buck circuit is observed; this is the current that flows through the coils of the SCR-1; this current is measured at the amperemeter *Am1*. Finally, Figure 11c also presents a graph of the voltage measured in the SCR-1 coils over time.

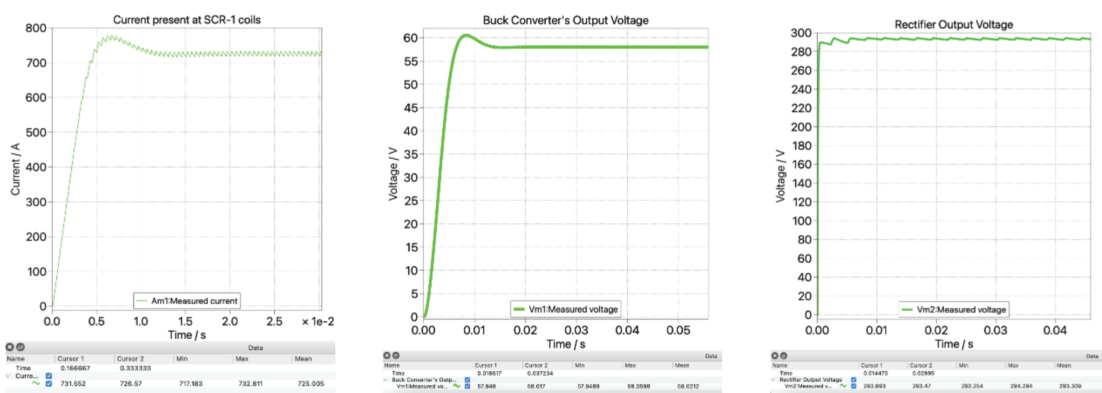

(a) (b) (c)

Figure 11. Rectified signals and measurements for: (a) Output voltage of the rectifier circuit, (b) current measured at the SCR-1 coils and (c) voltage measured at the SCR-1 coils.

Vlasov antenna for the ECRH system

To simulate the electric field generated by the coils shown in Figure 12a, Figure 12b was generated using the line drawing technique.

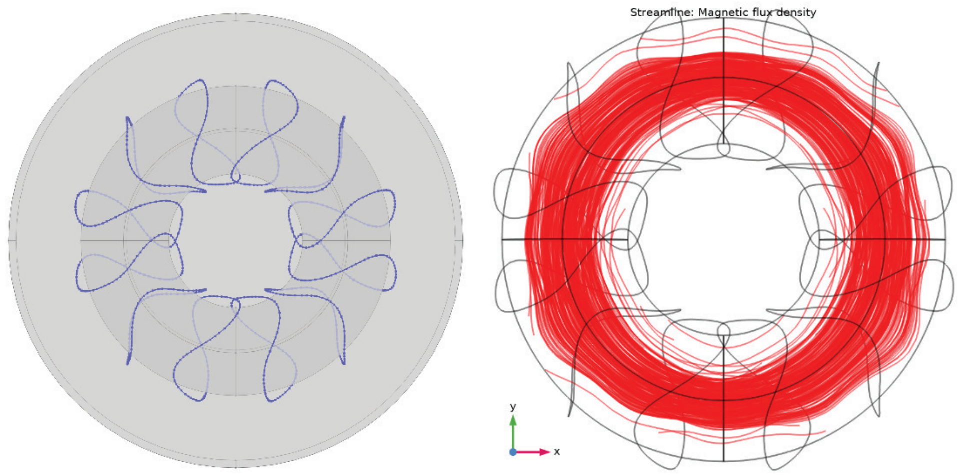

(a) (b)

Figure 12. (a) SCR-1 plasma containment field coils. (b) Magnetic flux density lines of the plasma containment system.

In the heating system, electromagnetic waves were utilized to determine the electric field magnitude. This visualization enabled observation of the path of electromagnetic waves within the SCR-1 vacuum vessel, illustrated in Figure 13, for different configurations.

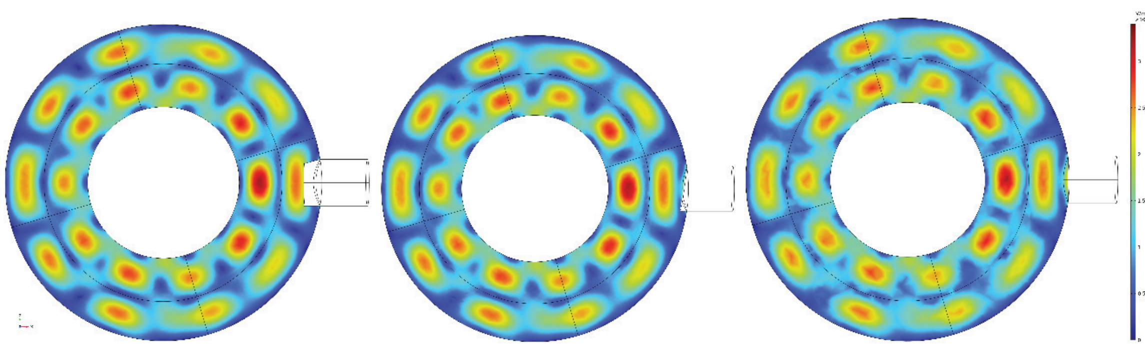

(a) (b) (c)

Figure 13. Magnitude of the electric field inside the SCR-1 vacuum vessel for (a) modified cut, (b) bevel-cut, (c) without the antenna.

In the laminar flow module describing the gas injected into the SCR-1 vacuum vessel, the inlet port where the gas is injected and the outlet port corresponding to the vacuum pump were defined. This resulted in the pressure surface shown in Figure 14.

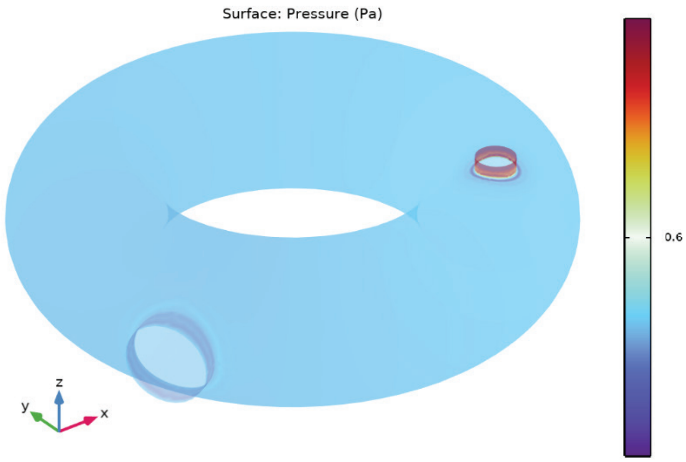

Figure 14. Pressure surface of laminar flow of the gas injected into the SCR-1 vacuum vessel.

Discussion and conclusions

In general, turbulence flow modes (common to all stellarator topologies) cannot be ruled out such as Electron Temperature Gradient modes, Ion Temperature Gradient modes, Trapped Electron Modes and drift waves, all of them affected by the action of the electrode with positive results and mitigated to a lesser or greater extent with the action of the induced shear flux. The effective use of a function generator and transformer in the electrode circuit design highlights the importance of precise control over frequency and amplitude in experimental plasma physics. Circuit simulation confirmed the successful implementation of these requirements, with observed signal characteristics aligning with design specifications. It was demonstrated that the implementation of an electrode in the SCR-1 stellarator effectively modulates plasma turbulence and behavior, particularly near the LCMS regions and SOL. These findings are consistent with those reported by [4], who highlighted that turbulence propagation is predominantly active near the SOL region. The electrode-induced electric field significantly reduced ion saturation current and altered electron density, providing valuable insights into turbulence dynamics. The decrease in radial velocity and particle flux near the LCMS upon electrode introduction underscores the electrode's impact on plasma confinement and turbulence suppression, as shown in Figure 9. These findings are consistent with previous studies, confirming that external electric fields can influence plasma characteristics and enhance confinement, as reported by [3].

Using the *PLECS* software, the proposed design for the circuits of the stellarator SCR-1 coils current control system was successfully verified, as shown in Figures 11a, 11b, and 11c. Regarding the full-wave rectifier, an AC input with an RMS voltage of 120 V was applied. The diode rectifier operated as expected, converting the AC signal into a pulsating DC signal. Figure 11a demonstrated how the capacitor smoothed the rectifier output, significantly reducing voltage ripple and improving signal stability. Proper filtering is essential to minimize fluctuations in the output voltage of the Buck converter. The voltage ripple of the rectifier circuit, as shown in Figure 11a, is approximately 1.5 V, equivalent to 0.5% of the input voltage. For the Buck converter circuit, Figure 11b shows that the average stabilized current is 725.012 A, with a ripple of 15.642 A, corresponding to 2.16% of the inductor current. Both values are suitable for the intended application. Additionally, in the same figure, the stabilization time of the circuit is approximately 0.02 s, which is acceptable for the stellarator application, where the discharge cycle is 8 s. Figure 11c displays the voltage value set to achieve the coil operating current, which also stabilizes within a very short period (0.02 s).

Using COMSOL Multiphysics software, a comprehensive simulation of SCR-1 was developed, integrating modules such as the electromagnetic wave module for the heating system and the laminar flow module for gas injection. By comparing the three cases depicted in Figure 13, a parametric sweep revealed that the modified cut case 45º improved the maximum electric field magnitude by up to 8%, while the bevel-cut case improved it by 9% with an angle of 81.4º, compared to the scenario without an antenna. This adjustment facilitated a more even spatial distribution. The reduction in wave reflection through the same port in the bevel-cut configuration contributed to these outcomes. Considering the geometry of the SCR-1 vacuum vessel, the optimized angle ensures a more uniform wave deposition within the SCR-1 vacuum vessel. The successful implementation of the 3D model of the SCR-1, including the parameterized Vlasov antenna with adjustable cutting angles, enabled the visualization of electromagnetic wave deposition within the SCR-1 by examining the electric field magnitude across different antenna configurations.

Future work should explore the effects of different electrode potentials and configurations to further understand their influence on plasma behavior. Additionally, extending the mapping of radial variations and SOL width will provide a more comprehensive understanding of turbulence dynamics and confinement in stellarator plasmas, contributing to the broader understanding of plasma turbulence control and offering practical insights for optimizing plasma confinement in fusion devices. Suitable cooling systems such as large heat sinks, fans, or liquid cooling should be designed and implemented to effectively manage thermal energy dissipation. Before the implementation of the power circuit and its respective control, lower power tests should be conducted using lower voltage batteries, gradually increasing to ensure safe operation. To enhance cost-effectiveness, designing several buck converters in parallel connection rather than a single unit can reduce the current requirements for each converter and lower costs. Utilizing thick copper traces and ground planes will accommodate high currents in the circuit PCB design. Future work will also involve testing additional antenna designs to analyze their behavior with the heating system once the plasma module is fully implemented, optimizing the interaction between the antenna and the SCR-1 plasma.

Acknowledgements

The authors gratefully acknowledge the financial support provided by the *Vicerrectoría de Investigación y Extensión (VIE)* of the Costa Rica Institute of Technology (Tecnológico de Costa Rica) under Research Project No. 5401-1450-1801.

References

[1] F. Coto-Vílchez *et al.*, “Progress on the small modular stellarator SCR-1: new diagnostics and heating scenarios”, *Journal Of Plasma Physics*, vol. 86, n.º 4, Jul. 2020, doi: 10.1017/s0022377820000677.

[2] O. E. Garcia, R. Kube, A. Theodorsen, and H. L. Pécseli, “Stochastic modelling ofintermittent fluctuations in the scrape-off layer: Correlations, distributions, level crossings, and moment estimation”, *Physics Of Plasmas*, vol. 23, n.º 5, May 2016, doi: 10.1063/1.4951016.

[3] N. Bisai and A. Sen, “Theory of plasma blob formation and its numerical andexperimental validations”, *Reviews Of Modern Plasma Physics*, vol. 7, n.º 1, Jun. 2023, doi: 10.1007/s41614-023-00124-5.

[4] G. Grenfell *et al.*, “Measurement and control of turbulence spreading in the scrape-off layer of TJ-II stellarator,” *Nuclear Fusion*, vol. 59, no. 1, p. 016018, Nov. 2018, doi: 10.1088/1741-4326/aaf034.

[5] M. Ramisch, F. Greiner, N. Mahdizadeh, K. Rahbarnia, and U. Stroth, Observation oflarge-scale coherent structures under strongE×Bshear in the torsatron TJ-K, *Plasma Physics and Controlled Fusion*, vol. 49, no. 6, pp. 777–789, Apr. 2007, doi: 10.1088/0741-3335/49/6/006.

[6] J. Bergman, “Surface-mountable dual-polarized antenna arrays for 100 GHz,”, Masterthesis, *Dept. of Electronics and Nanotechnology,* Aalto University, Finland, Mar. 21, 2022. https://urn.fi/URN:NBN:fi:aalto-202203272551

[7] R. Solano-Piedra, "Simulación de escenarios de calentamiento por microondas paraconocer las condiciones de la propagación de ondas de Bernstein electrónicas en el plasma del stellarator SCR-1". Master's thesis, *Universidad de Costa Rica*, Sistema de Estudios de Posgrado, Ciudad Universitaria Rodrigo Facio, Costa Rica.

[8] F. Fanale *et al.*, "Progress on the conceptual design of the antennas for the DTT ECRHsystem," *Fusion Engineering and Design*, vol. 192, p. 113797, May 2023, doi: 10.1016/j.fusengdes.2023.113797.

[9] A. Köhn *et al.*, "Schemes of microwave heating of overdense plasmas in the stellaratorTJ-K," *Plasma Physics and Controlled Fusion*, vol. 55, no. 1, p. 014010, Dec. 2012, doi: 10.1088/0741-3335/55/1/014010.

[10] H. Zhou and X. Yang, "Design of Novel VLASOV-type Antennas for High Power Microwaves (HPM)," *2007 IEEE 34th International Conference on Plasma Science (ICOPS)*, p. 912, Jun. 2007, doi: 10.1109/ppps.2007.4346218.

[11] H. M. E. Misilmani, M. Al-Husseini, and K. Y. Kabalan, "Improved Vlasov Antenna with Curved Cuts and Optimized Reflector Position and Shape," *International Journal of Antennas and Propagation*, vol. 2015, pp. 1–12, Jan. 2015, doi: 10.1155/2015/193630.

[12] D. Jiménez, L. Campos-Duarte, R. Solano-Piedra, L. A. Araya-Solano, E. Meneses, and I. Vargas, BS-SOLCTRA: Towards a parallel magnetic plasma confinement simulation framework for modular stellarator devices, *in Proc. High Performance Computing: 6th Latin American Conf. (CARLA 2019)*, Turrialba, Costa Rica, Sept. 25–27, 2019, *Revised Selected Papers*, vol. 6, pp. 33–48, 2020.

[13] J. Boedo *et al.*, "Enhanced particle confinement and turbulence reduction due to E B shear in the TEXTOR tokamak," *Nuclear Fusion*, vol. 40, no. 7, pp. 1397–1410, Jul. 2000, doi: 10.1088/0029-5515/40/7/309.

[14] J. Mora, I. Vargas, and J. Asenjo, Diseño de un regulador de corriente eléctrica para las bobinas modulares del Stellarator SCR-1, *Revista Tecnología En Marcha*, vol. 30, no. 5, p. 21, Dec. 2017, doi: 10.18845/tm.v30i5.3220.

[15] N. Mohan, T. M. Undeland, and W. P. Robbins, *Power Electronics: Converters, Applications, and Design*. 2003.

[16] H. Trimino, "Design of an ech system for a small modular stellarator," *2011 Abstracts IEEE International Conference on Plasma Science*, p. 1, Jun. 2011, doi: 10.1109/plasma.2011.5993156.

Statement on the Use of Artificial Intelligence (AI)

The AI tool *Google NotebookLM* was used to support the organization of literature, the synthesis of reference documents, and the enhancement of the manuscript's writing clarity. All generated or suggested content was reviewed and validated by the authors prior to its incorporation into the article.